

# Insight into the GPS Navigation Product Accuracy using the SLR measurements

Mark A. Davis, \*  
Aaron J. Trask, †

August 18, 2007

## Overview

There has been a slow trend of increasing agreement between the a posteriori navigation products (SP3 Ephemeris) produced by the Radio Frequency (RF) community and the Satellite Laser Ranging (SLR) measurements. However, there still remain differences which can not be explained. This paper summarizes the location of the tray of corner cube reflectors on the Global Positioning System (GPS) 35 and 36 satellites, demonstrates the seasonally systematic residual differences in the line of sight measurements, shows the utility of the nearly simultaneous SLR measurements, and summarizes the potential sources of the remaining discrepancy. Until these are resolved, it is believed that the remaining structure is being needlessly absorbed into the clock estimates and remains one of the largest terms in the user error budget [1, 2]. Recent attempts to demonstrate the fidelity of the RF signal and earth dynamic models as shown in References [3, 4, 5, 6, 7, 8, 9] demonstrate the impact of International Earth Rotation Service (IERS) conventions adoption amongst the various RF production processes [10]. The systematic differences between adopted, realized and recommended [11, 12] practices are making noticeable differences in the improvement of these RF based products as measured by the sparse but accurate SLR measurements.

## Introduction - Overall Statistics

Table 1 is a summary of the agreement between the RF Navigation products (IGS, JPL, CODE, NGS), which are a representative subset of the International Global Navigation Satellite System (GNSS) Service (IGS) contributions as computed from the available SLR measurements. All of these were obtained from the Crustal Dynamics Data Information System (CDDIS) and span the Modified Julian Days (MJD) 53600 thru 54302, so as to reflect the most current and accurate products available. The data in the table were constructed using batches of 50 days where the SP3 formatted trajectories have been converted to the Naval Research Laboratory (NRL) internal format and moved to the UTC timescale. The SLR normal-points (converted to Merit2 for convenience) are then used to generate the residuals and the assorted conditions of the measurement using the LASEROMC software. The output is then screened at the 0.10 meter level for the tabulation. Nominal Local-Vertical-Local-Horizontal (LVLH) attitude for the satellites is assumed and new estimates of the optical reflection point were used. Details and remaining uncertainty for the SV retroreflector locations are shown in the section "TRAY LOCATION". The majority of the SLR station positions are from the ITRF2000 [13], while those not available were corrected using short arc fits to Laser Geodynamics Satellite (LAGEOS) fits with core ITRF2000 located stations. Also, hybrid weights on the sites were used with the process documented [14] for NRL's SLR based reference catalog. No ocean or atmospheric loading affects on site displacement were implemented in the residuals computed for this paper, however some comments on this issue are included.

---

\*Naval Research Laboratory, Code 8123, Electro-Optics Technology Sections, Honeywell Technology Solutions, Inc., Washington D.C. 20375

†Naval Research Laboratory, Code 8125, Astrodynamics and Navigation Section, Washington D.C. 20375

source	GPS35 mean meters	GPS35 rms meters	GPS35 samples	GPS36 mean meters	GPS36 rms meters	GPS36 samples
IGS	-0.0160	0.0244	8418	-0.0139	0.0266	7071
JPL	-0.0159	0.0279	8377	-0.0166	0.0289	6960
CODE	-0.0225	0.0236	8457	-0.0221	0.0268	7071
NGS	-0.0129	0.0261	8339	-0.0056	0.0278	7009

Table 1: Summary of the one way range comparison between RF Navigation Products and the SLR Measurements spanning MJD 53600 through 54302 (Aug 18 2005 - July 21 2007).

Both the Center for Orbit Determination in Europe (CODE) and the Jet Propulsion Laboratory (JPL) routinely compare their RF based ephemeris with the SLR measurements [53, 52]. The JPL results are graphical reported and are not directly numerically comparable. The CODE produces a daily report "GNSS Quick-Look Residual Analysis Report" measuring the agreement from their rapid navigation product and the SLR measurements. The tabular pass averages from these reports were compared to the statistics shown in Table 1. The differences found were related to the editing criteria (0.01 meters and 10 point normal-points) and RF product computation latency (Rapid vs Final). A fair comparison using the first half of year 2006 [15] to compare the CODE Final ephemeris with the SLR measurements resulted in a mean difference of 0.009 meters and 0.005 meters on GPS 35 and 36, with standard deviations differing by less than 0.0020 meters. This comparison was made prior to the (August 2006) changes to the operational residual software at CODE marking a very notable improvement in the routinely reported agreement of the SLR and GPS techniques. Updates to these comparisons now that a longer timeseries has been sampled could be performed.

Shown in Figure 1 is the timeseries of the NRL generated residuals with a very clear and systematic residual pattern. This is a unusually long and densely supported SLR tracking interval for a fourteen day interval in early 2004. The conventional way to describe the location of the satellite in the orbit plane as a function of solar season is a useful way to map these residuals to a correlation argument. The nomenclature requires a reference angle (omega) such that orbit midnight is -90 degrees and noon is +90 degree with the two other cardinal points being at equator crossings. Examination of the recent dataset shows this pattern (see Figure 2 and 3) where the argument is the reference angle omega. An additional unrelated residual pattern occurs during the midnight region during the eclipsing season when the attitude yaw turn occurs.

The correlation with solar season does vary with time, and can further be explained by breaking the dataset into beta prime intervals. The estimation of function with the form Amplitude \* sin (omega + phase) + bias was performed over several intervals. This technique was first performed over January 2000 thru August 2004, where the coefficients were estimated. These are also included for comparison. These are illustrated in Figure 4 and summarized for each producer and shown in Table 2 and 3 for the interval [53600 to 53945] and a longer series from the original estimation. The final ephemeris from the IGS, JPL, CODE and US National Geodetic Survey (NGS) were included to show the variability of the various production organizations. These were chosen to make direct comparison to other analysis and to illustrate systematic differences among the IGS. The overall mean is naturally zero for functions of this form, with remaining RMS of 0.0156 and 0.0182 meters for GPS 35 and 36 when no eclipse season data are assessed.

The dataset which has been observed after the estimation interval has been used assess the stability of these values. The residuals when this function is fitted to the IGS GPS35 data result in mean 0.0055 with RMS 0.0237 meters and for the IGS GPS36 data result in mean 0.0099 with RMS 0.0207 meters suggesting a non stationary process.

This functional form is hoped to be used by others to explain this systematic difference. Unlike trying to use the sparse SLR measurements, this continuous form of the signal should be usable by the RF navigation and clock community. Recent (Sept 2006) SLR mail #1493 [16] suggest that Chapter 7 of the "IERS Conventions on Displacement of reference points" has clarification of implementation ambiguity which may be measurable by these techniques.

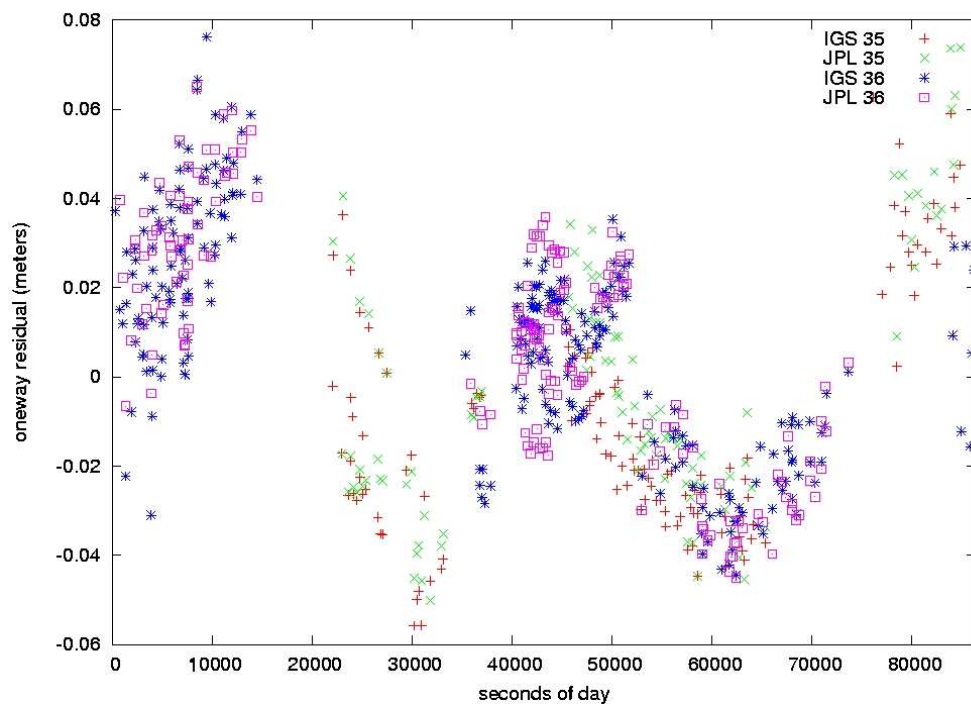


Figure 1: SLR residuals for GPS 35 and 36 from two weeks in January 2004 as a function of seconds of day for the IGS final and JPL final ephemeris

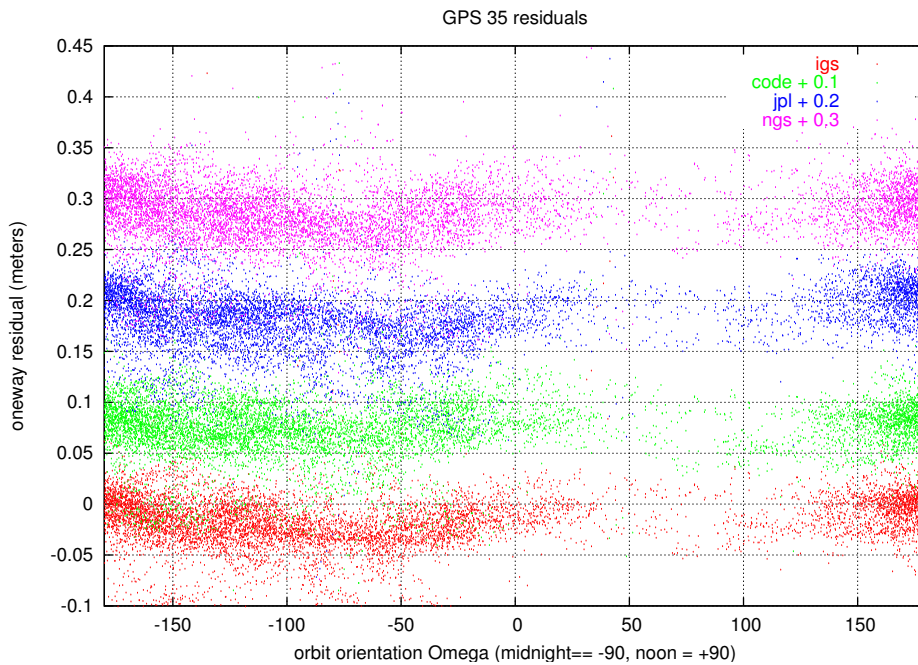


Figure 2: SLR residuals as a function of orbit angle (degrees) with each series shifted by 0.10 meters for clarity for GPS35 from (53600 .. 54302).

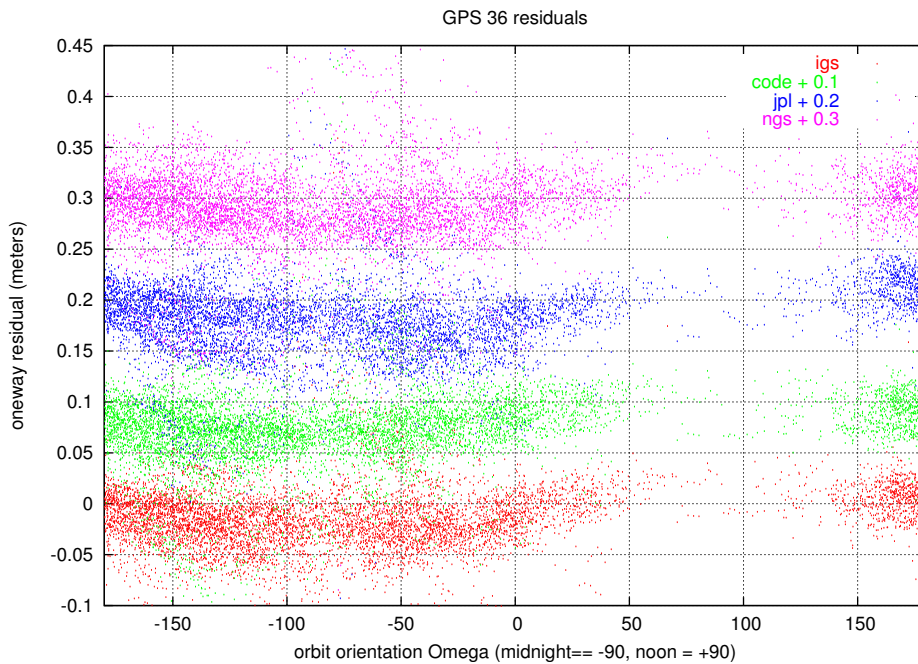


Figure 3: SLR residuals as a function of orbit angle (degrees) with each series shifted by 0.10 meters for clarity for GPS35 from (53600 .. 54302).

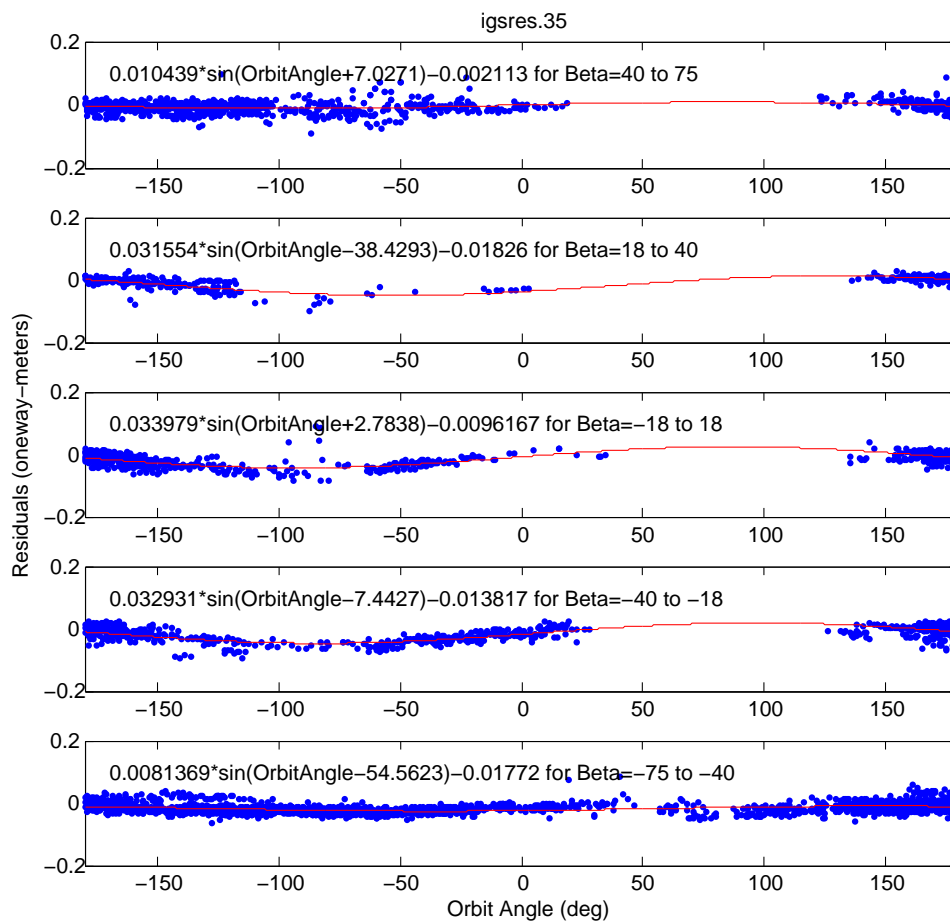


Figure 4: Example of the estimation of trend for beta prime regions for GPS 35

source	beta prime	amplitude	phase	bias
igs.35 2000-2004	bin 60 to 80	0.0074	0.0	-0.0116
igs.35 2000-2004	bin 40 to 60	0.0124	0.0	-0.0105
igs.35 2000-2004	bin 20 to 40	0.0248	0.0	-0.0118
igs.35 2000-2004	bin 0 to 20	0.0254	0.0	-0.0144
igs.35 2000-2004	bin -20 to 0	0.0410	0.0	-0.0148
igs.35 2000-2004	bin -40 to -20	0.0289	0.0	-0.0159
igs.35 2000-2004	bin -60 to -40	0.0144	0.0	-0.0174
igs.35 2000-2004	bin -80 to -60	0.0032	0.0	-0.0186
igs.35	bin 40 to 75	0.0104	+7.0271	-0.0021
ngs.35	bin 40 to 75	0.0179	+15.4451	+0.0023
cod.35	bin 40 to 75	0.0098	+56.2677	-0.0133
jpl.35	bin 40 to 75	0.0130	-4.8904	-0.0031
igs.35	bin 18 to 40	0.0315	-38.4293	-0.0183
ngs.35	bin 18 to 40	-0.0286	+92.7933	-0.0261
cod.35	bin 18 to 40	0.0167	-29.2622	-0.0217
jpl.35	bin 18 to 40	-0.0400	-153.0384	-0.0110
igs.35	bin -18 to 18	0.0340	+2.7838	-0.0096
ngs.35	bin -18 to 18	0.0042	+49.0682	-0.0107
cod.35	bin -18 to 18	0.0269	+13.9674	-0.0148
jpl.35	bin -18 to 18	0.0422	-10.4575	-0.0087
igs.35	bin -40 to -18	0.0329	-7.4427	-0.0138
ngs.35	bin -40 to -18	0.0184	-6.2864	-0.0098
cod.35	bin -40 to -18	0.0282	-0.99086	-0.0233
jpl.35	bin -40 to -18	0.0281	-17.9124	-0.0127
igs.35	bin -75 to -40	0.0081	-54.5623	-0.0177
ngs.35	bin -75 to -40	0.0093	-48.3175	-0.0185
cod.35	bin -75 to -40	-0.0036	+58.6303	-0.0300
jpl.35	bin -75 to -40	-0.0071	+100.1055	-0.0107

Table 2: GPS 35 Coefficients of Trend Estimates (MJD spanning [53600..53945]).

source	beta prime	amplitude	phase	bias
igs.36 2000-2204	bin 60 to 80	0.0072	0.0	-0.0001
igs.36 2000-2204	bin 40 to 60	0.0121	0.0	-0.0055
igs.36 2000-2204	bin 20 to 40	0.0571	0.0	+0.0069
igs.36 2000-2204	bin 0 to 20	0.0416	0.0	-0.0002
igs.36 2000-2204	bin -20 to 0	0.0521	0.0	-0.0095
igs.36 2000-2204	bin -40 to -20	0.0211	0.0	-0.0109
igs.36 2000-2204	bin -60 to -40	0.0186	0.0	-0.0076
igs.36 2000-2204	bin -80 to -60	0.0125	0.0	+0.0035
igs.36	bin 40 to 75	0.0177	+18.4231	+0.0039
ngs.36	bin 40 to 75	0.0225	+18.2467	+0.0119
cod.36	bin 40 to 75	0.0183	+38.0816	-0.0157
jpl.36	bin 40 to 75	0.0159	-11.0143	-0.0056
igs.36	bin 18 to 40	0.0413	+2.8798	-0.0090
ngs.36	bin 18 to 40	0.0098	+18.3495	-0.0064
cod.36	bin 18 to 40	0.0468	+14.8089	-0.0131
jpl.36	bin 18 to 40	0.0422	-9.0613	-0.0055
igs.36	bin -18 to 18	0.0474	+1.8604	-0.0066
ngs.36	bin -18 to 18	0.0101	+29.8247	-0.0025
cod.36	bin -18 to 18	0.0438	+4.1314	-0.0175
jpl.36	bin -18 to 18	0.0569	-4.8448	-0.0066
igs.36	bin -40 to -18	0.0331	-14.2031	-0.0129
ngs.36	bin -40 to -18	0.0104	-13.3274	-0.0029
cod.36	bin -40 to -18	-0.0142	+167.1574	-0.0188
jpl.36	bin -40 to -18	-0.0276	+149.6552	-0.0123
igs.36	bin -75 to -40	0.0185	-25.1984	-0.0040
ngs.36	bin -75 to -40	-0.0247	+144.2488	-0.0005
cod.36	bin -75 to -40	-0.0154	+151.4861	-0.0160
jpl.36	bin -75 to -40	-0.0150	+124.3346	-0.0058

Table 3: GPS36 Coefficients of Trend Estimates (MJD spanning [53600..53945]).

## Tray Location

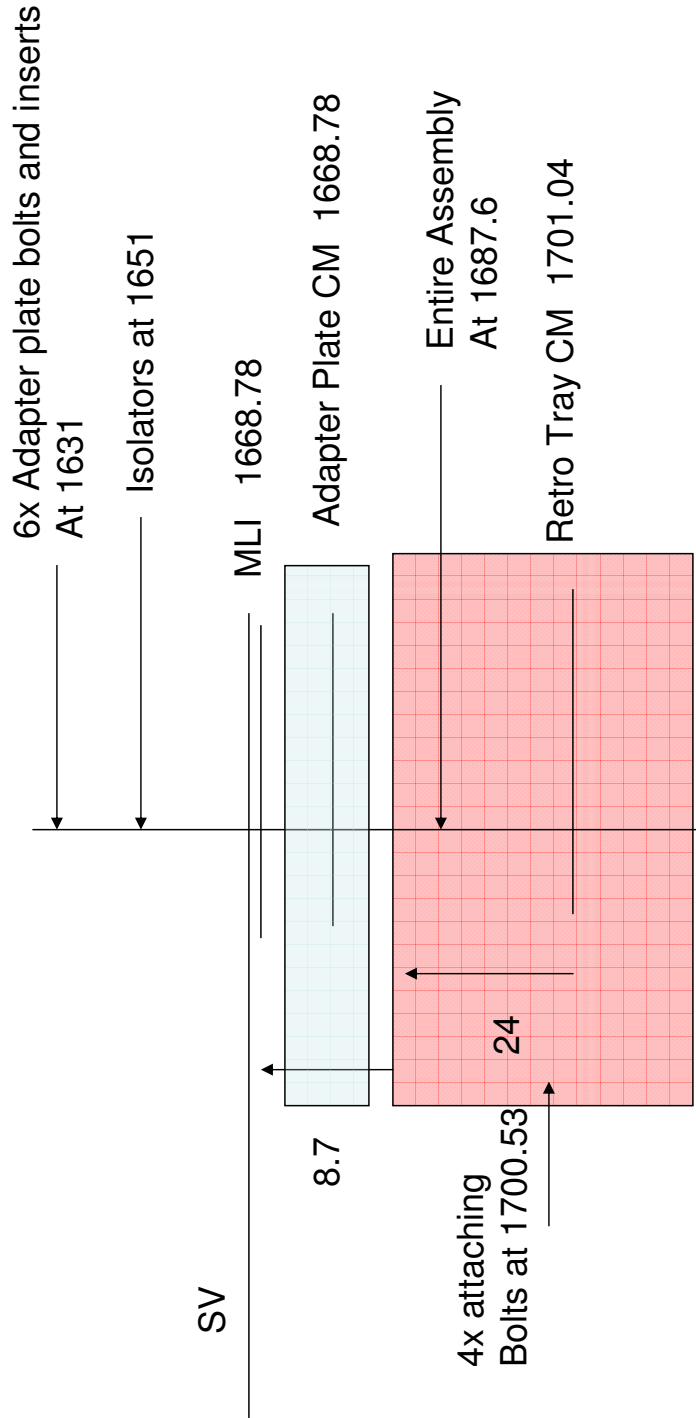
The documentation supporting the tie between the optical reflection plane and the satellite center of mass was revisited. The additional clarification of the flight stack of materials and the details from the Westpac retroreflector holders permits the computation of optical reflection point with respect to several items' center of mass. The mass properties documentation does have a detail item, which has been used by the community [17] up until now. This has been in error due to the naming convention of the components. The mass properties documents were examined with information shown [18, 19, 20] in the Figures 5 and 6. There was an additional adapter plate installed as shown in Figures 5 and 6. The Z component locations spanning the vicinity [1631..1701.04 millimeters ] are measured in the SV frame for a number of mechanical components of interest and are shown in Figure 5. Current estimates of the center of mass of the the SV in this frame are (0.0,0.0,1013.6) and (0.0,0.0,1011.3) for GPS 35 and 36 respectively, with an uncertainty of 3 mm for the Z component. These figures have measurements which have been augmented by the addition detail of the corner cube holder shown in the Westpac documentation [21]. There are many measurements which indicate that these are identical to those used as documented in [22], with the exception of the vertex dimensional tolerance being symmetric on the GPS tray, and asymmetric on the Westpac corner cubes which are bounded by a millimeter.

The computed distances from the Fixation Plane (mounting surface) and the vertex were computed in [22] to be the 7.1 millimeters for normal and 5.8 for 13 degrees incidence (20 degrees SLR observing site elevation). Another method of the computation is to start from the SV location of the MLI film. This location, and the mechanical distances to the aperture of the corner cubes can be computed ( $-24.0 + 37.0 - 1.5 - 18.93 * 1.4607 = -16.15$ ). Thus the optical reflection plane is closer to the CM of the SV than the CM of the tray and is 7.84 mm from the mounting surface. This is assuming that the CM of the tray is 24 millimeters from the mounting surface.

The new recommended values for the geometric center of the tray and the optical reflection plane (862.58, -524.51, 669.5 mm) for GPS35 and (862.58, -524.51, 671.7 mm) for GPS36 at normal incidence. The difference is the tabular center of mass locations in the respective body frame. Any systematic azimuth dependence on the incident angle should average out in the normal point formation process.

This value should be adjusted for incidence angle and potentially signal strength and pulse width considerations.

### Details of the Center of Mass Reported Line Items



Adapter plate is likely 10" x 8" at 1.795 lbs thus at least 0.228 " thick Aluminum  
 Or a lighter material or not solid to make up 3 mm

Units are millimeters from SV cm

Figure 5: Center of Mass Detail for the tray of reflectors on GPS 35 and 36

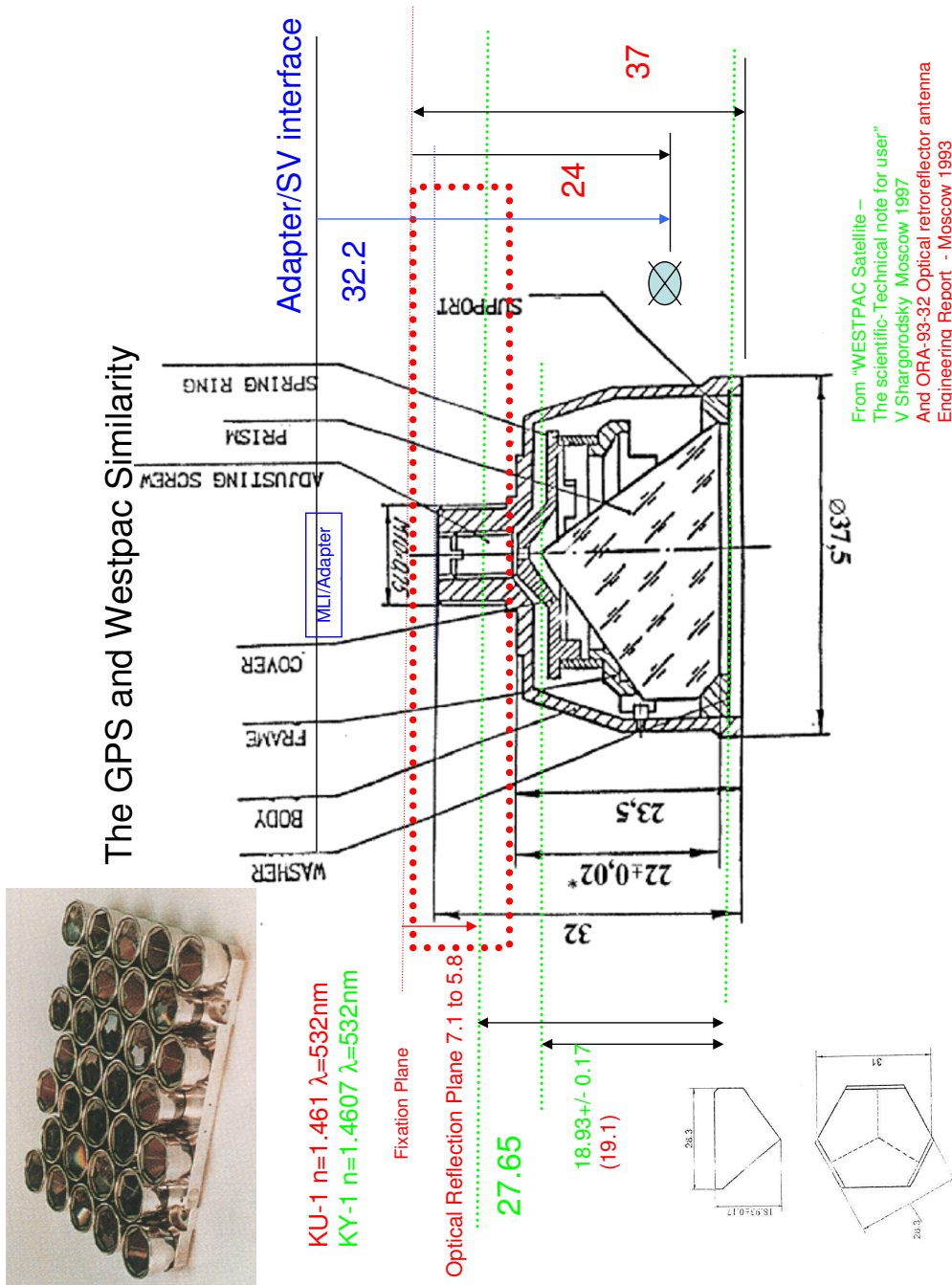


Figure 6: Optical Phase Center relationship to the CM of the tray of reflectors on GPS 35 and 36

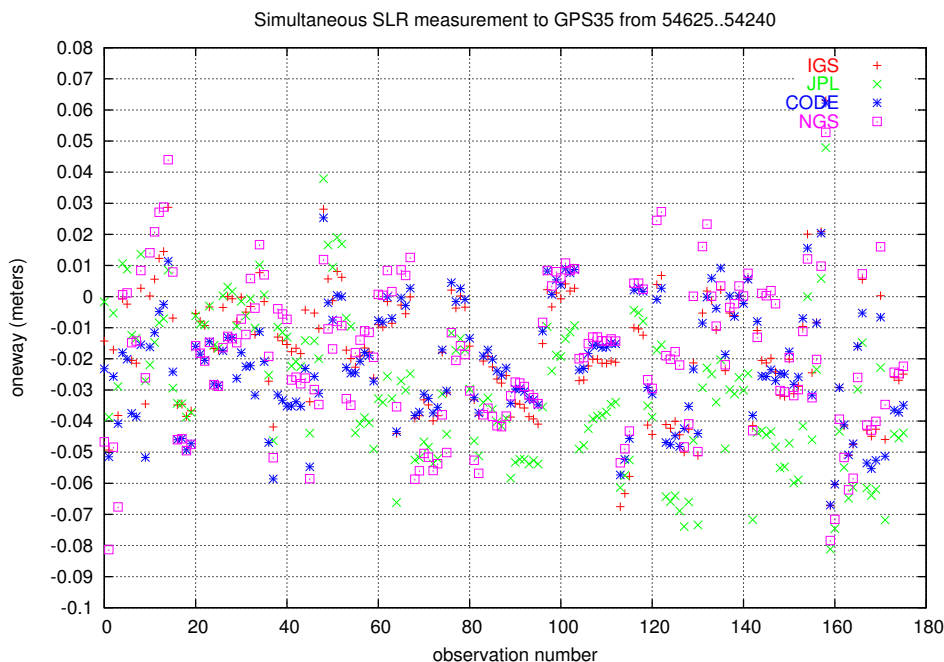


Figure 7: Simultaneous SLR observations illustrate differing behavior in the IGS contributors for GPS 35.

## Near Simultaneous Observations

The orbit errors of these satellites (which are slowly varying) can be assessed over intervals of a half hour without loss in significance. Knowing that much of this error is at the one cycle per revolution [24] we can observe 3 percent of the amplitude ( $10/360 * 12$  hrs) in this interval. This is the same underlying assumption behind the use of normal points by the SLR community instead of the raw full rate observations, but extended in duration to strengthen the available dataset. The archives of data were assessed from 1993:309 thru 2007:213 for GPS35 and 1994:114 thru 2007:217 (year:day of year). Any measurement which has been reported was included for a total of 43 sites and 48372 normal point observations for GPS35 and 42 sites and 40261 normal point observations for GPS36, spanning the 5018 and 4853 day interval. The times when three or more sites reported normal points in the same 30 minute interval are shown in summary form in Table 4. Details of these are shown in Appendix Table 6, 7, 8 and 9. These tables have ILRS pad identifiers followed by the number of raw points included in the five minute normal points for the interval. The 2006 study includes some of these nearly simultaneous observations where there are 0.1 meter biases included in Figure 7 and 8 to illustrate that there is remaining structure among the individual navigation solutions under assessment.

The very nature of a geometric solution would suggest that all the modeling would have the residuals exceedingly tiny. However, in this is not the case. The data represents a set for directly scoring the improvement in the RF models.

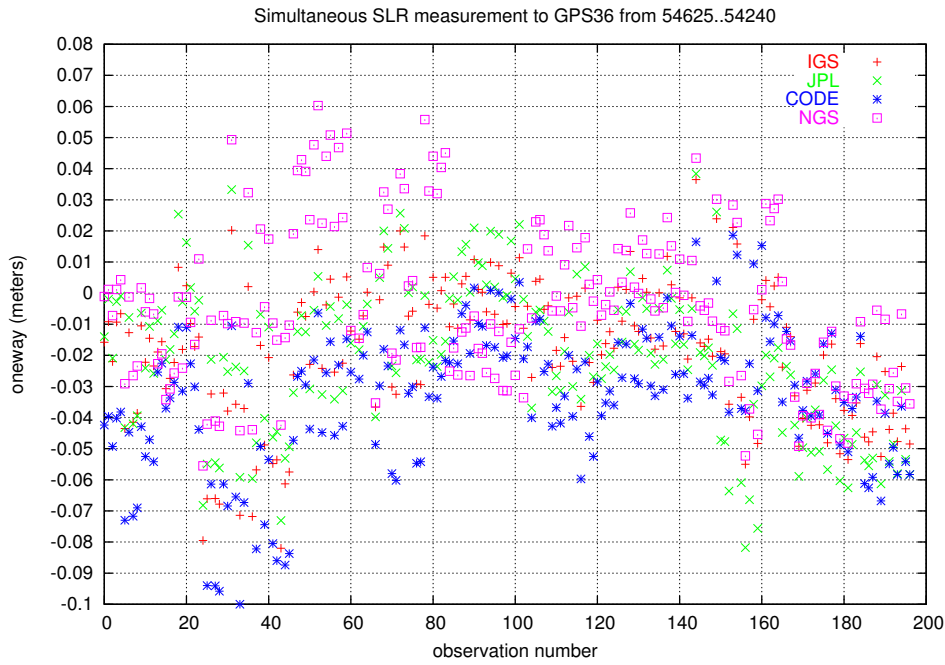


Figure 8: Simultaneous SLR observations illustrate differing behavior in the IGS contributors for GPS 36.

Site	35 events	36 events
7210	13	7
7080	12	2
7110	10	10
7884	4	1
7109	1	0
7105	3	7
7918	0	9
7839	68	59
8834	48	25
7840	40	35
7810	39	42
7832	38	39
7845	26	20
1864	3	6
7941	8	8
1884	2	0
7835	2	3
7841	1	1
7811	2	0
1893	0	2
1873	0	1

Table 4: Occurrences by site for simultaneous ranging dataset.

## Accuracy Budget

The overall potential for errors is shown in Table 5. Given the established one cycle per revolution difference between the navigation products and the SLR measurements, it should not be a surprise that orbits which fit the SLR measurements (typical precision is under 8 mm RMS over weeks) will not agree with the RF solutions. A simple radial bias of 0.020 meters will map to orbit differences with magnitude 0.05 radial, 0.37 intrack, 0.42 crosstrack or 0.57 meters RMS [26]. Much of the contributions in Table 5 are specific to the NRL Optical Test Facility, which is tied to GGAO [25] and the official WGS84 [26, 27] through the DoD and IGS GPS receivers at the US Naval Observatory (USNO). However the errors could be generalized for the ILRS SLR systems on the global scale with likely tighter tolerances. Most of the terms characterize the Line of Sight (LOS) from the ground observatory and the satellite. Assessments of the Atmospheric and Ocean Loading are rough estimates [28, 29]. The bulk of the SLR measurements have been made at elevations greater than 45 degrees, and the improvements in the Pavlis et al [30] will be small, but the 12 degree statistic is shown to upperbound any summary.

Nonconservative Force modeling has received periodic investigation[31, 24, 41, 37, 32, 33, 15, 34, 38], and steady improvement for the bulk of the operational life of this mission. The strength in the SLR measurement and the ability to fit weeks [42, 43] or months [17] with reasonable agreement with independent data arcs (fit vs predicts) suggest there remain improvement in the modeling with the RF observations. Longer arcs or more dense datasets could confirm this, however the repeat overflight geometry and the tendency for observations only high in elevation (a function of the current retro array small cross section) are leaving untapped capability of the SLR network.

## Future Work

While the mission to date dataset for GPS 35 and 36 is sparse compared with that of the RF receivers, there is sufficient confidence in the results and direct evidence of overall quality of the RF solutions and the evidence of systematic ephemeris and modeling errors. There is also tremendous value to the independent orbit determination in having the overflight geometry fall between and not directly over the site (as is the case for GPS36 where GGAO can see both the eastern and western over flights, when Maui tracked thru the midnight turn, and when YARRAGADEE and MT. Stromlo can see both sides of the noon turn) when there is a fixed repeat ground track.

Investigations into the multi discipline technique can be explored using the removal of the sinusoidal residual pattern shown here during the orbit determination process over longer arcs when processing RF only solutions. Additionally, the coordinated gathering on all the GNSS mission of nearly simultaneous data will make the exploitation and analysis of future datasets more readily useful in bringing the RF and Laser community measurements into agreement in hopes of better understanding the clocks and the Earth dynamics.

## Acknowledgement

The results presented here depend upon the observations and products of the ILRS [46] and the IGS [47]. The support of all the contributions is gratefully acknowledged. The mass properties documents obtained in support of the NGA Accuracy Improvement Initiative [40] were instrumental in resolving the tray location.

## References

- [1] Suni Bisnath, Richard Langley, "Precise a posteriori Geometric Tracking of Low earth Orbiters with GPS", Canadian Aeronautics and Space Journal - submitted 1999.
- [2] C. Urschl, G. Beutler, W. Gurtner, U. Hugentobler, S. Schaer, "GPS/GLONASS orbit determination based on combined microwave and SLR data analysis".
- [3] Urs Hugentobler, "Models in GNSS Data Analysis", COMET 2005, November, London.

ERROR SOURCE CONTRIBUTIONS	Component	LOS Range Impact	Note
<b>GPS SPACE VEHICLE SEGMENT</b>			
GPS Pitch/Roll Attitude Control	Z	17.6 mm per degree	0.5 deg (spec)
GPS Yaw Attitude Control	X and Y	17.4 mm per degree	0.5 deg (spec)
GPS Yaw Attitude Control	Z	3.9 mm per degree	0.5 deg (spec)
Geodetic vs Geocentric Pointing	Z	0.8 mm	0.045 deg
Reported Center of Mass Precision	Z	2.5 mm	0.1 inch (table precision)
<b>SLR RETROREFLECTOR TRAY</b>			
Optical Phase Center Uncertainty	Z	1.3 mm peak	multiple retro aperture effect
Leading/Trailing Edge vs Middle of Tray for Single Photon Collection	LOS random	+/- 34 mm	averaged by normal point formulation process
<b>SLR GROUND STATION</b>			
SLR System Delay Uncertainty	LOS	10 mm RMS	detectable on calibration targets
SLR Meteorological Data Uncertainty	LOS	0.7 mm	0.1 mBar, 0.2 deg K, 10 percent at 20 deg
Telescope Location	LOS	max 6.0 mm	site position survey tie to ITRF
Telescope Location Rate	LOS	max 0.2 mm /year	ITRF velocity uncertainty
Reference Frame	LOS	max 10.0 mm	site position WGS84/ITRF at USNO
Atmospheric Loading	LOS	2 mm max	site height
<b>ENVIRONMENTAL</b>			
Troposphere Model Bias	LOS	< 2.3 mm	at 1064 nm
Troposphere Accuracy	LOS random	< 12 mm	random at 20 deg elevation
		20 degrees elevation	averaged by np process
Ionospheric Model	LOS	0.0 mm	zero at optical wavelengths
Geocenter Motion	LOS	10 mm maximum	site position

Table 5: Error sources for the navigation product accuracy assessment

- [4] C. Urschl, W. Gurtner, U. Hugentobler, S. Schaer, G. Beutler, "Validation of GNSS orbits using SLR observations", *Advances in Space Research*, 35, 2005, 412-417.
- [5] G.M. Appleby, T. Otsubo, "Comparison of SLR Measurements and Orbits with GLONASS and GPS Microwave orbits".
- [6] G.M. Appleby, T. Otsubo, "Evaluation of Potential Systematic Bias in GNSS Solutions", 13th ILRS workshop.
- [7] Graham Appleby, Toshimichi Otsubo, "Laser Ranging as a Precise Tool to Evaluate GNSS Orbital Solutions", 14th International Laser Ranging Workshop, San Fernando, Spain, June 7-11 2004.
- [8] Michael J. Merrigan, Everett R. Swift, Robert F. Wong, Joedy T. Saffel, "A Refinement to the World Geodetic System 1984 Reference Frame", Institute of Navigation, ION-GPS-2002, Portland, OR, September 2002.
- [9] James O'Toole, Michael Merrigan, "Evaluation of DoD GPS Satellite Orbits Using NASA Laser Ranging Data", ION 199[5/6] 45-54.
- [10] J. Ray, D. Dong, Z. Altamimi, "IGS Reference Frames: Status and Future Improvements", AIUB workshop and Symposium "Celebrating a Decade of the IGS".
- [11] *IERS Technical Note 21, IERS Conventions (1996)*, McCarthy, D., U.S. Naval Observatory, July 1996.
- [12] *IERS Technical Note 32, IERS Conventions (2003)*, McCarthy, D., Petit, G., Nov 2003.
- [13] *IERS Technical Note 31, The 2000 International Terrestrial Reference Frame (ITRF2000)*, Boucher, C., Altamini, Z., Sillard, P, Feissel-Vernier, M. (editors), 2002.
- [14] John Seago, Mark Davis, Anne Clement, "Precision of a Multi-Satellite Trajectory Database Estimated from Satellite Laser Ranging" AAS/AIAA Space Flight Mechanics Meeting, Clearwater FL, Jan 2000, AAS 00-180
- [15] Claudia Urschl, G. Beutler, W. Gurtner, U. Hugentobler, S. Schaer, "Validation of GNSS orbits using SLR observations", IGS Workshop 2006, may, ESOC Darmstadt Germany.
- [16] Jim Ray, SLR MAIL 1493 and IERS Message 87, 2006.
- [17] J.J. Degnan, E.C. Pavlis, "Laser Ranging to GPS Satellites with Centimeter Accuracy", *GPS World*, September, 1994.
- [18] Philip Mendicki, Aerospace Corp, "35,36 Mass Properties 2004-02-25.xls", study personal communications, email 06-May-2004.
- [19] subset of "Updated Mass Properties Report", 30-aug-1993
- [20] subset of "Updated Mass Properties Report", 02-mar-1994
- [21] V. Shargorodsky, "WESTPAC Satellite, The Scientific-Technical note for user", Moscow 1997.
- [22] Russian Institute for Space Device Engineering, "Optical retroreflector antenna ", Engineering Report ORA-93-32, Moscow 1993.
- [23] "Optical Retroreflector Antenna", ORA-93-32, Engineering Report of the Russian Institute for Space Device Engineering, Moscow 1993.
- [24] Oscar L. Colombo, "The Dynamics of Global Positioning system Orbits and the Determination of Precise Ephemerides", *Journal of Geophysical research*, Vol 94, no b7, 9167-9182, July 10, 1989.
- [25] Alan Hope, Jay Middour, Joseph Simons, Mark Davis, Jacques Fein, "Establishment and Validation of the NRL One-Meter Telescope Position," AAS 04-239, 14th AAS/AIAA Space Flight Mechanics Meeting, Maui, HI, Feb. 8-12, 2004.

- [26] Mark Davis, Aaron Trask, Jay Middour, Alan Hope, Chris Moore, William Scharpf, Reed Smith, Michelle, Suite, Harris Ray Burris, Mena Stell, "NGA GPS Navigation Accuracy Assessment using SLR Techniques", Unpublished NRL Report, 2004.
- [27] Department of Defense World Geodetic System 1984, NIMA TR8350.2, 3rd Edition, Ammendment1, 3 January 2000.
- [28] Leonid Peltrov, Jean-Paul Boy, "Study of the atmospheric pressure loading signal in very long baseline interferometry observations", *Journal of Geophysical Research*, Vol 109, B03405, 2004, doi:10.1029/2003JB002500.
- [29] Helen Phillips, Jeff Ridgway, Jean-Bernard Minster, Donghui Yi, Charles Bentley, "Geoscience Laser Altimeter System (GLAS), Tidal Corrections", Algorithm Theoretical Basis Document, Version 2.0, August 1999.
- [30] V. Mendes, G. Prates, Erricos Pavlis, D. Pavlis, R. Langley, "Improved mapping functions for atmospheric refraction correction in SLR"
- [31] H.F. Fliegel, T. Gallin, E. Swift, "Global Positioning System Radiation Force Model for Geodetic Applications", *Journal of Geophysical Research*, Vol 97 No B1, 559-568, January 10, 1992.
- [32] Yvonne Vigue, Stephen M. Lichten, Ron J. Mullerschoen, Geoff Blewitt, Michael B. Heflin, "Improved GPS Solar Radiation Pressure Modeling for Precise Orbit Determination", *Journal Of Spacecraft and Rockets*, Vol 31, No 5, pages 830-833, Sept-Oct 1994.
- [33] Yoaz Bar-Sever, "A New Model for Yaw Attitude of Global Positioning System Satellites", JPL TDA Progress Report 42-123, pages 37-46, November 15, 1995.
- [34] D. Kuang, H.J. Rim, B.E. Schutz, P.A.M. Abusali, "Modeling GPS attitude variations for precision orbit determination", *Journal of Geodesy*, Vol 70, number 9, pages 572-580, 1996.
- [35] Yoaz Bar-Sever, D. Kuang, "New Empirically-Derived Solar Radiation Pressure Model for GPS Satellites", *European Geophysical Society* 2003, Vol 5.
- [36] ARINC Research Corporation, "NAVSTAR GPS Space Segment/Navigation User Interfaces", ICD-GPS-200, Revision C, 10 Oct 1993 with IRN-200C-[001-004] 12 Apr 2000.
- [37] Eanes, R., Nerem, R., Abusali, P., Bamford, W., Key, K., Ries, J., Schutz, B., "GLONASS Orbit Determination at the Center for Space Research," published PDF form on ILRS Internet webpage, link on <http://ilrs.gsfc.nasa.gov/GLONASS>
- [38] Ivan Georgeiv, "GPS orbit determination by SLR data", Bulgarian Academy of Sciences, <http://geosat.cc.bas.bg/GPS35.htm>.
- [39] Stephen Malys, Margaret Larezos, Steven Gottschalk, Shawn Mobbs, Bryant Winn, William Feess, Michael Menn, Everett Swift, Michael Merrigan, William Mathon, "The GPS Accuracy Improvement Initiative", (*Ion .gt.* 1997 ) 375-384.
- [40] Tom. Creel, Arthur Dorsey, Philip Mendicki, Jon Little, Richard Mach, Brent Renfo "New, Improved GPS, The Legacy Accuracy Improvement Initiative ", *GPS World*, March 2006, pp 20 - 31.
- [41] Yoaz Bar-Sever, "New GPS attitude model", IGS mail 0591, May 9, 1994.
- [42] Richard S. Hujsak, G. Charmaine Gilbreath, "Sequential Orbit Determination For GPS-35 and GPS-36 using SLR data from NRL@SOR", *SPIE Proceedings*, 3380 (32), Orlando, April 1998.
- [43] Richard S. Hujsak, G. Charmaine Gilbreath, Son Truong, "GPS Sequential Orbit Determination Using Sparse SLR Data",
- [44] G. Charmaine Gilbreath, Mark A. Davis, "NRL Ranging Accuracy Analysis for NRL@SOR SLR Capability", *SPIE Proceedings*, 3380 (29), Orlando, April 1998.

- [45] Mark A. Davis, G. Charmaine Gilbreath, Peter Rolsma, Jamie, Georges, Gregg Snyder, Richard eichinger, "NRL@SOR SLR Observation Techniques Using LAGEOS", Proceedings 11th International Workshop on Laser Ranging, Deggendorf, September 1998.
- [46] M. Pearlman, J. Degnan, J. Bosworth, "The International Laser Ranging Service", Advances in Space Research, Vol 30, No 2, 135-143, July 2002.
- [47] G. Beutler, M. Rothacher, S. Schaer, T.A.Springer, J. Kouba, R.E. Neilan, "The International GPS Service (IGS): An interdisciplinary Service in Support of Earth Sciences", Advances in Space Research, Vol 23, No. 4, 631-635, 1999.
- [48] John Degnan and Erricos Pavlis, " Laser Ranging to GPS Satellites with Centimeter Accuracy ", GPS World , pages 62-70, September 1994.
- [49] Gerald Mader, Frank Czopek, " The Block IIA Satellite Calibrating Antenna Phase Centers" GPS World , pages 40-46, May 2002.
- [50] John Seago, David Vallado, "Coordinate Frames of the US Space Object Catalogs", AIAA/AAS Astrodynamics Specialist Conferenct, AIAA 2000 - 4025, Denver, CO, August 14-17, 2000.
- [51] Tim Springer, " routine igs product from CODE "
- [52] JPL website for the SLR residuals.
- [53] CODE periodic GNSS Report, <http://cdis.gsfc.nasa.gov/reports/slrcode/slrgps/YYYY>.

## Appendix - Simultaneous Observations

Tables 6, 7, 8, 9 are those intervals of less than 30 minutes with geometric solutions. The number of fullrate points in each normal point are included.

MJD	Site1	Site2	Site3	Site4
49332.4458	7080 29	7210 11	7105 6	
49332.4561	7080 14	7210 6	7105 4	
49332.4626	7080 34	7210 4	7110 160	7105 1
49332.4775	7080 4	7210 11	7110 209	
49332.4881	7080 2	7210 11	7110 214	
49987.5084	7080 10	7210 2	7110 23	
50014.4875	7080 161	7109 1	7110 97	
50386.3802	7080 4	7210 3	7884 297	
50386.3897	7080 94	7210 10	7884 136	
50398.4785	7210 1	7110 17	7884 53	
50398.4802	7210 5	7110 1	7884 69	
50426.3168	7080 118	7210 11	7110 7	
50430.3517	7080 113	7210 19	7110 30	
50430.3546	7080 1	7210 6	7110 3	
50692.9775	7839 49	7840 45	1884 24	
50692.9877	7839 84	7840 137	1884 33	
50707.9475	7839 25	7840 22	8834 171	
50707.9668	7839 17	7840 15	8834 350	
51376.9752	7839 14	7840 55	7810 33	
51384.9723	7839 5	8834 266	7810 13	
51384.9809	7839 11	8834 223	7810 4	
51388.9883	7839 56	8834 53	7811 8	
51388.9953	7839 101	8834 11	7810 22	
51389.9477	7839 75	8834 128	7810 26	
51389.954	7839 119	8834 175	7810 7	
51389.9645	7839 22	8834 94	7810 40	
51438.8944	7840 23	1864 60	7845 626	
51715.0279	7839 125	7840 50	7835 17	
51715.0387	7839 8	7840 38	8834 20	
51715.0505	7839 107	7840 36	8834 121	
51717.0496	7839 10	8834 73	7810 15	
51717.0608	7839 5	8834 122	7810 18	
51766.8954	7839 73	7840 77	8834 99	
51780.9471	7840 11	8834 83	1864 4	
52105.9567	7840 9	7845 262	7835 260	
52117.9265	7839 6	7840 8	7810 6	
52117.9364	7839 20	7840 34	7810 3	
52128.8728	7839 27	7810 54	7845 351	
52135.8838	7839 149	7840 14	7810 55	
52135.8936	7839 27	7810 69	7845 294	
52455.9774	7839 27	7832 919	7845 152	
52455.9834	7839 12	7832 32	7845 113	
52487.912	7839 15	7840 17	7810 11	
52548.7492	7839 7	1864 92	7832 224	
52792.0532	8834 79	7832 392	7841 14	
52813.9467	7840 31	7832 37	7845 1072	
52813.9569	7840 78	7832 169	7845 839	
52814.9216	7840 20	7810 40	7845 253	
52820.9285	7839 32	7840 170	7845 216	
52820.9681	7839 20	7840 6	7845 92	
52826.9673	7840 35	7832 161	7845 263	
52826.9731	7840 41	7832 10	7845 302	
52827.9145	7840 45	7832 351	7845 158	

Table 6: Nearly Simultaneous ranging for GPS 35 (part 1 of 2). Column entries are ILRS identifier and number of raw points in the normalpoint

MJD	Site1	Site2	Site3	Site4
52827.9236	7840 39	7832 104	7845 20	
52829.9148	7840 37	7810 24	7845 520	
52829.9237	7840 31	7810 11	7845 11	
52838.9468	7839 42	7810 4	7845 340	
52845.9044	7839 32	8834 14	7832 352	
52845.9112	7839 44	8834 41	7832 268	
52854.8642	7839 35	7832 240	7845 269	
52854.8735	7839 8	7832 275	7845 151	
52855.8517	7839 27	7832 476	7845 127	
52855.8626	7839 6	7832 657	7845 134	
52870.7893	8834 109	7832 238	7845 398	
52870.7993	8834 97	7832 630	7845 63	
52877.78	7839 54	7832 400	7845 575	
52877.7854	7839 6	7832 236	7845 349	
53186.9285	7839 509	8834 75	7810 10	7941 478
53186.9451	7839 105	8834 6	7941 12	
53204.862	7839 298	8834 80	7832 110	7941 893
53204.8652	8834 15	7832 139	7941 329	
53539.9162	7839 835	7840 34	7832 37	7810 6
53539.9319	7839 120	7840 20	7832 13	
53542.9465	7839 371	7832 10	7810 63	
53625.6501	7839 426	7832 86	7810 25	
53639.6456	7839 899	7832 554	7810 10	
53846.9704	7840 17	8834 9	7810 3	
53893.8935	7839 176	8834 77	7941 25	
53893.8978	7839 307	7840 51	8834 317	7810 9
53897.8277	7839 1291	8834 30	7810 8	
53897.9135	7839 1157	8834 19	7832 24	
53898.9265	7839 234	7840 22	8834 19	7832 17
53983.6505	8834 143	7832 6	7810 46	
54171.0927	8834 68	7832 154	7810 44	
54171.0942	7840 63	7832 17	7810 12	
54199.9983	7839 107	8834 132	7810 47	
54202.0146	7839 110	8834 65	7810 7	
54202.0308	7839 1168	8834 113	7810 15	
54202.036	7839 2852	8834 21	7810 7	
54207.0178	7839 1213	8834 30	7810 7	
54207.0259	7839 457	8834 55	7810 18	
54207.0406	7839 591	8834 26	7810 15	
54207.9564	7839 596	7840 49	7941 25	
54210.9371	7839 594	7840 86	7941 57	
54210.946	7839 850	7810 38	7941 347	
54211.0181	7839 814	8834 6	7832 21	7810 6
54212.9777	7839 1091	8834 98	7832 9	
54212.9885	7839 801	7840 19	8834 6	7832 43
54217.9971	7839 374	8834 67	7832 6	
54221.9883	7840 28	8834 104	7832 67	
54222.9772	7839 342	7840 11	8834 180	
54222.9871	7839 543	7840 9	8834 41	
54239.9353	7839 153	7840 12	8834 52	
54240.9274	8834 22	7832 10	7811 3	

Table 7: Nearly Simultaneous ranging for GPS 35 (part 2 of 2)

MJD	Site1	Site2	Site3	Site4
50398.5226	7110 479	7210 11	7884 101	
50412.4882	7105 109	7210 3	7918 5	
50412.4947	7105 50	7210 4	7918 29	
50414.4679	7110 20	7210 3	7918 1	
50414.4761	7110 1	7210 8	7918 6	
50414.4872	7105 44	7110 1	7918 16	
50414.5083	7105 141	7110 100	7918 649	
50414.5189	7105 134	7110 73	7918 164	
50414.5289	7105 12	7110 82	7918 67	
50414.539	7105 323	7110 63	7918 68	
50436.4171	7080 222	7110 11	7210 2	
50436.4271	7080 87	7110 85	7210 2	
51164.7274	8834 94	7839 21	7845 1478	
51164.7364	8834 55	7839 257	7845 1122	7810 36
51184.7287	1864 15	7840 58	7839 26	
51193.6764	1864 35	7839 5	7845 162	
51389.0904	8834 112	7839 28	7810 49	
51389.097	8834 118	7839 27	7810 52	
51508.7798	8834 3	7839 12	7835 61	
51767.0299	7840 43	7839 11	7845 221	
51777.0296	7840 20	7839 17	7835 66	
51809.9253	7839 23	7835 54	7845 417	
51833.8638	8834 43	7840 6	7839 8	
52184.8903	7839 18	7845 37	7810 35	
52190.831	7839 20	1893 1	7845 486	
52190.8375	7839 16	1893 7	7845 72	
52217.7584	7840 17	7839 13	7845 315	
52548.8488	8834 98	7839 42	7845 326	
52597.7482	7839 6	7845 247	7832 115	
52826.0418	7840 69	7839 55	7832 5	
52826.9938	7840 100	7839 21	7845 178	
52839.0298	7840 63	7839 47	7832 262	
52839.0404	7840 47	7839 45	7832 122	
52839.061	7840 42	7839 38	7832 771	
52839.0679	7840 12	7845 19	7832 438	
52854.9775	7839 82	7845 359	7832 374	
52857.9876	7840 15	7839 68	7841 14	
52858.9139	7840 74	7839 64	7845 70	
52860.9144	7840 97	7839 27	7810 30	
52862.9986	8834 66	7840 6	7839 6	
52878.885	7839 56	7845 50	7810 5	
52886.9216	7840 10	7839 24	7845 252	

Table 8: Nearly Simultaneous ranging for GPS 36 (part 1 of 2)

MJD	Site1	Site2	Site3	Site4
52894.884	7840 30	7832 604	7941 112	
52894.8899	7840 18	7832 507	7941 47	
52899.8518	7840 30	7810 55	7941 318	
52899.8626	7840 42	7810 39	7941 388	
52905.8413	7840 35	7845 551	7832 306	
52924.7518	7832 18	7941 70	1873 1	
53177.0706	7840 23	7832 95	7941 232	
53256.7858	7839 250	7810 4	7832 69	
53256.8322	7839 530	7845 173	7810 19	
53256.8355	7839 566	7845 31	7810 29	
53283.7064	7839 972	7810 8	7832 129	
53540.0511	7840 61	7810 74	7832 7	
53544.9313	8834 11	7840 128	7810 32	
53554.9569	7839 942	7810 15	7832 10	
53554.9633	7839 815	7810 8	7832 15	
53554.9772	7839 2947	7810 6	7941 9	
53567.9373	7840 43	7810 8	7832 12	
53587.9149	7840 93	7839 473	7832 443	
53590.8838	7839 241	7810 26	7832 66	
53610.8526	7840 51	7810 6	7832 210	
53610.8613	7840 101	7810 8	7832 24	
53636.7228	8834 5	7839 341	7810 12	
53653.6683	8834 6	7810 42	7832 53	
53669.6959	1864 22	7810 24	7832 229	
53669.6983	1864 10	7810 14	7832 44	
53672.6912	1864 51	7810 4	7832 42	
53912.9462	7839 154	7810 6	7832 189	
53912.9552	7839 857	7810 10	7832 55	
53918.9427	1864 2	8834 111	7810 5	
53920.9462	8834 23	7840 56	7832 182	
53920.9488	8834 83	7840 49	7832 92	
53932.8974	7840 24	7839 219	7810 46	
53933.9462	7840 65	7839 440	7832 419	
53933.9567	7839 1111	7810 3	7832 422	
53933.9626	7839 888	7810 5	7832 191	
53934.9156	8834 154	7840 61	7810 13	
53940.9149	7839 1452	7810 6	7832 296	
53963.8165	8834 78	7839 300	7832 85	
54054.5715	8834 56	7839 493	7810 9	
54054.5816	8834 56	7839 926	7810 77	
54054.5923	8834 45	7839 229	7810 44	7237 4
54211.1082	8834 63	7840 16	7839 190	
54223.0226	8834 20	7840 25	7839 423	
54239.0612	7839 345	7810 20	7832 219	
54239.9988	8834 33	7839 1032	7832 19	
54240.0151	7839 514	7810 6	7832 46	
54240.0297	8834 94	7839 237	7810 14	
54240.0413	8834 37	7839 292	7810 6	
54294.8629	8834 37	7839 544	7810 44	
54294.8934	7839 283	7832 87	7941 11	

Table 9: Nearly Simultaneous ranging for GPS 36 (part 2 of 2)